6th International Conference on Advances in Experimental Structural Engineering
11th International Workshop on Advanced Smart Materials and Smart Structures Technology
August 1-2, 2015, University of Illinois, Urbana-Champaign, United States

Vibration Characteristics of Mountable PZT Interface on Tendon Anchorage Connection

T.C. Huynh[1], K.S. Lee[2], J.T. Kim[3]

1, PhD Student, Smart Structures Engineering Laboratory, Pukyong National University, Busan, Korea.
E-mail: ce.huynh@gmail.com.
2, MS Student, Smart Structures Engineering Laboratory, Pukyong National University, Busan, Korea.
E-mail: isca88@gmail.com.
3, Professor, Smart Structures Engineering Laboratory, Pukyong National University, Busan, Korea.
E-mail: idis@pknu.ac.kr.

ABSTRACT
In this paper, local vibration characteristics of mountable PZT interfaces are numerically analyzed to verify their feasibility for impedance-based prestress-loss monitoring in tendon anchorage connections. Firstly, a prestressed tendon-anchorage connection with mountable PZT interfaces is described. Two types of mountable interfaces which are different in geometric and boundary conditions are designed for impedance monitoring in the tendon-anchorage. Secondly, laboratory experiments are conducted to evaluate the impedance monitoring via the two mountable PZT interfaces installed on the tendon-anchorage under the prestress force variation. Frequency-shifts and root-mean-square-deviations are utilized to quantify the change of impedance signatures for the two PZT interfaces. Finally, local dynamic characteristics of the two PZT interfaces are numerically analyzed to verify their performances on impedance monitoring at the tendon-anchorage system. For the two PZT interfaces, the relationships between structural parameters and local vibration responses are examined by modal sensitivity analyses. Peak impedance responses and their corresponding vibration parameters sensitive to the prestress force variation are identified by analyzing local vibration characteristics and experimentally measured impedance responses.

KEYWORDS: *Local dynamic, PZT interface, tendon anchorage, prestress force, modal sensitivity*

1. INTRODUCTION

Damage detection in structural systems via monitoring impedance signatures has been studied by many researchers (Liang et al. 1996, Zagrai and Giurgiutiu 2001, Bhalla and Soh 2003). The 'so-called' impedance-based method utilizes the electro-mechanical (EM) impedance of a coupled PZT (Lead Zirconate Titanate)-structure system to identify the change in dynamic characteristics at the local structural region. Recently, the impedance-based method has been applied for monitoring the prestress-loss in tendon-anchorage connections (Kim et al. 2010, Nguyen and Kim 2012, Huynh and Kim 2014). A limitation of their studies was on setting the frequency band sensitive to the variation of the prestress forces. The effective frequency band was even over 800 kHz for a mono-tendon anchorage under compressive forcing about 100 kN (Kim et al. 2010). To overcome the disadvantage, Nguyen and Kim (2012) developed an impedance-sensitive PZT interface technique which could reduce the frequency band to below 100 kHz and also the need of a high performance impedance analyzer. However, this design of PZT interface should be installed during the construction of the anchorage subsystem, so it is impossible to apply it into existing joint members.

In order to overcome the above-mentioned drawbacks, Huynh and Kim (2014) proposed a portable PZT interface that could be mounted on (and detached from) the surface of bearing plates. The proposed PZT-interface technique was experimentally evaluated for a lab-scaled cable structure to monitor the change in impedance responses caused by the change in prestress forces. Also, a numerical impedance analysis was conducted to examine the performance of a new interface device (Huynh et al. 2014). Despite those research attempts, however, there still exists a need to verify the feasibility of monitoring impedance responses via the portable PZT interface mounted on the bearing plate that is subjected to the variation of the anchoring forces. In other words, the relationship between the anchor force and the structural response of the PZT interface should be proved in order to justify the mountable PZT interface-based impedance monitoring of the prestress-loss.

In this study, local dynamic characteristics of mountable PZT interfaces are numerically analyzed to verify their feasibility on impedance monitoring of the prestress-loss in the tendon anchorage subsystems. The relationships

between structural parameters and local vibration responses of the interfaces are examined by modal sensitivity analyses. Peak impedance responses and their corresponding structural parameters sensitive to the variation of prestress forces in the anchorage subsystem are identified by analyzing local dynamic characteristics and experimentally measured impedance responses.

2. TENDON-ANCHORAGE CONNECTION WITH MOUNTABLE PZT INTERFACE

2.1. Two Types of Mountable Interfaces

The mountable PZT interface is designed to monitor EM impedance signatures of the prestressed tendon-anchorage system. As shown in Figure 2.1, the PZT interface is mounted on the bearing plate that is subjected to the variation of the anchoring forces. For tendon-anchorage systems, the effect of the bearing plate on the interface's local resonance is assumed to be negligibly small. This assumption comes from the fact that the PZT interface has much smaller flexural stiffness than the bearing plate. In this study, the PZT interface is designed to deal with 1V-amplitude excitation and impedance monitoring using wireless sensor technology which allows the frequency range of 10-100 kHz (Mascarenas et al. 2007). The PZT interface's structural properties are basically selected to fulfill the limitation of the wireless impedance monitoring.

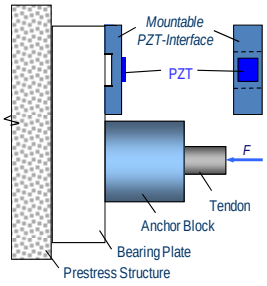

Figure 2.1 Prestressed tendon-anchorage system with a mountable PZT-interface

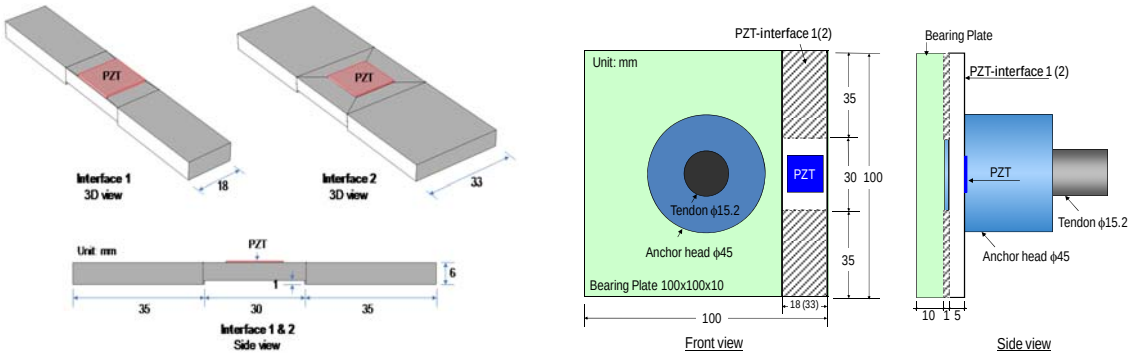

(a) Geometries of two interfaces (b) Geometries of tendon-anchorage (Huynh et al. 2014)

Figure 2.2 Geometries of tendon-anchorage equipped with mountable PZT interfaces

For experimental verification, two types of PZT interfaces were designed to examine their performances for impedance monitoring. Figure 2.2(a) shows the two interfaces and their geometries. The aluminum interfaces have the fixed-fixed boundary condition by two outside contact bodies and the flexible beam section in the middle, as shown in the side view. The fixed boundary conditions are simulated by contact surfaces bonded on the bearing plate. The fixed sections of the two interfaces have the following dimensions: 35x18x6 mm^3 (Interface 1) and 35x33x6 mm^3 (Interface 2). The unbonded beam sections, where the PZTs are installed, are designed to allow flexural vibration responses and piezoelectric deformation in longitudinal and lateral directions. The unbonded sections have the following dimensions: 30x18x5 mm^3 (Interface 1) and 30x33x5 mm^3 (Interface 2). It is noted that the bonding area of Interface 2 is larger (about 1.8 times) than that of Interface 1. As shown in Figure 2.2(b), the PZT interfaces are installed at the right end of the bearing plate of the tendon-anchorage system. A mono-tendon of ϕ15.2 mm is anchored by an anchor head of ϕ45 mm on the bearing plate of 100x100x10 mm^3. The material properties of the tendon-anchorage, the PZT interfaces, and the

EM properties of PZT-5A patch are referred to the existing publication (Huynh et al. 2014).

2.2. Impedance Measurement via Two Interfaces

Laboratory experiments were carried out for a tendon-anchorage system with the two mountable PZT-interfaces (i.e., Interfaces 1 and 2) as shown in Fig. 2.3. A tendon cable of 6.4 m was anchored by bearing plates at both ends. Tension force was introduced into the cable by a stressing jack as the cable was anchored at one end and pulled out at the other. A load cell was installed at one tendon-anchorage to measure the actual cable force. For each test, the PZT patch on the interface was excited by a harmonic excitation voltage with 1V-amplitude, and the impedance signature was measured by an impedance analyzer HIOKI 3532. The tendon cable was first pre-tensioned to T1 = 49.05 kN and reduced into T2 = 39.2 kN, T3 = 29.4 kN and T4 = 19.6 kN for prestress-loss simulation.

Figure 2.3 Lab-scaled tendon-anchorage connection with two PZT interfaces

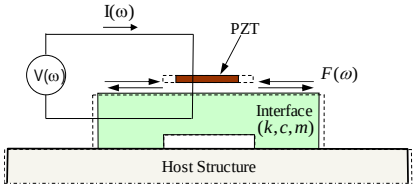

Figure 2.4 PZT-interface-structure model for structural impedance response

Impedance responses of the two PZT interfaces were measured in the frequency range 10-100 kHz. The frequency range was examined to evaluate the feasibility of the two PZT interfaces on impedance monitoring using wireless technology which allows only the frequency range of 10-100 kHz (Mascarenas et al. 2007). In practice, the electric current I(ω) is measured and utilized to calculate the electromechanical (EM) impedance which contains the structural mechanical (SM) impedance (Liang et al. 1996). As shown in Figure 2.4, the SM impedance can be explained from the interaction between the PZT patch and the structure (e.g., the interface body). An input harmonic voltage V(ω) induces a deformation of the PZT due to the inverse piezoelectric effect. Then a force F(ω) against that deformation is induced into the structure (i.e., the interface bodies) and the PZT as well, because the PZT is surface-bonded to the interface structure. The SM impedance is defined as the ratio of force to velocity as follows (Liang et al., 1996):

$$Z_s(\omega) = \frac{F(\omega)}{\dot{u}(\omega)} = c + m\frac{\omega^2 - \omega_n^2}{\omega} i \tag{2.1}$$

where c and m are the damping coefficient and the mass of the interfacing structure with the PZT patch, respectively; ω_n is the angular natural frequency of the interface structure; and ω is the angular frequency of the excitation voltage. As shown in Eq. (2.1), the SM impedance is a function of structural properties (i.e., mass, damping, and stiffness), so that the change in structural parameters can be inversely interpreted by the change in the SM impedance.

3. IMPEDANCE MONITORING PERFORMANCE OF TWO INTERFACES

3.1. Impedance Responses of Two Interfaces

The performances of impedance monitoring via the mountable PZT interfaces were examined for the prestress

forces T1 – T4. Figure 3.1(a) shows real impedance signatures of Interface 1 in the wide frequency range 10-100 kHz (901 interval points) and the two narrow resonant bands of 18-21 kHz (Peak 1, 501 interval points) and 81-84 kHz (Peak 1, 501 interval points) for the four cases of prestress force T1-T4. For Interface 2, real impedance signatures in the frequency range 10-100 kHz (901 interval points) and two resonant frequency bands of 14-20 kHz (Peak 1, 501 interval points) and 34-40 kHz (Peak 2, 501 interval points) are shown in Figure 3.1(b). For the two PZT interfaces, it is observed that both Peak 1 and Peak 2 are varied as tendon forces decrease. This implies that the contribution of the SM impedance to the EM impedance is considerable in the resonant frequency ranges, as explained in Eq. (2.1).

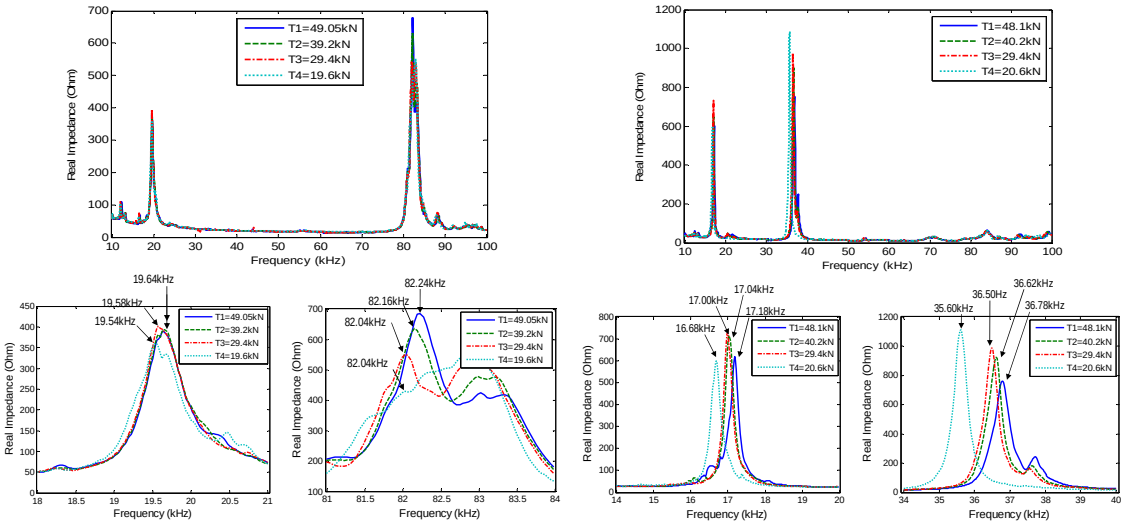

(a) Interface 1 (b) Interface 2

Figure 3.1 Impedance responses measured from Interfaces under various forces

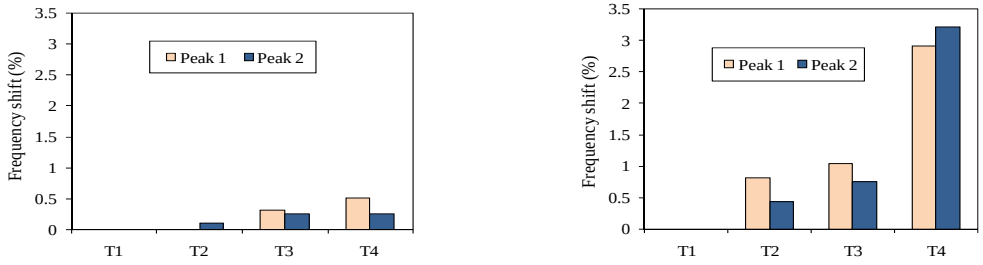

(a) Interface 1 (b) Interface 2

Figure 3.2 Frequency shifts measured from Interfaces 1 and 2 under various forces

As shown in Figure 3.1, the resonant frequencies tend to shift left, according to the decrement of the tendon force. This indicates that the modal stiffness of the interfaces is decreased with the reduction of the tendon force. As shown in Figure 3.2, when the tendon force is reduced about 60% from T1-T4, the peak frequencies of Interface 1 shift very small, not greater than 0.5% for the first resonant frequency (f_1) and 0.2% for the second one (f_2) while the those of Interface 2 shift relatively high as 2.8% for the first resonant frequency (f_1) and 3.2% for the second one (f_2).

3.2. RMSD Index of Two Interfaces

Generally, RMSD is sensitive to both horizontal shift and vertical shift of impedance signature. As observed in Figure 3.1, the change in tendon forces causes not only vertical shift but also horizontal shift of impedance responses as measured by Interface 1. Therefore, RMSD indices are examined for four tension levels. Figures 3.3 and 3.4 show RMSD indices calculated according to the increment of tendon force-loss for the two narrow frequency ranges corresponding to the two peak impedance responses of Interfaces 1 and 2. For Interface 1, the RMSD indices increase gradually as the tendon forces are reduced from T1 to T4. The RMSD indices of the second peak's frequency range (i.e., 81-84 kHz) show a little more sensitive indication of tension-loss than that of the first peak's frequency range (18-21 kHz). For Interface 2, the RMSD indices increase

proportionally as the tendon forces are reduced from T1 - T4. The RMSD indices of the first peak's frequency range (i.e., 14-20 kHz) and those of the second peak's frequency range (i.e., 34-40 kHz) show both very sensitive indications of the tension-loss. The RMSD indices of Interface 2 indicate the structural changes about 5-10 times more sensitively as compared to those of Interface 1. This result indicates that Interface 2 can better detect the change in impedance responses due to the loss of tension forces.

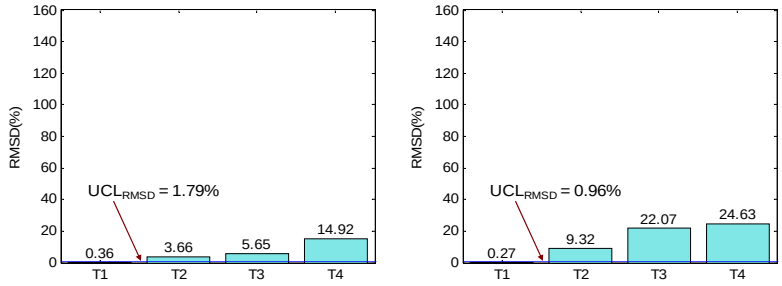

(a) Peak 1 (18-21 kHz) (b) Peak 2 (81-84 kHz)
Figure 3.3 RMSD index of Interfaces 1 under various forces

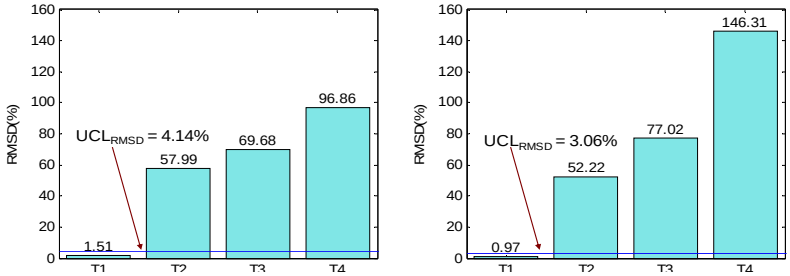

(a) Peak 1 (14-20 kHz) (b) Peak 2 (34-40 kHz)
Figure 3.4 RMSD index of Interfaces 2 under various forces

4. DYNAMIC CHARACTERISTICS OF MOUNTABLE PZT INTERFACES

Dynamic characteristics of the two PZT interfaces are examined to understand the relationship between structural properties of the interfaces and their sensitive resonant frequencies of impedance signatures. Note from Figure 3.1 that the impedance signatures in the non-resonant regions 21-81 kHz (Interface 1) and 20-34 kHz (Interface 2) are almost unchanged due to the change of tendon forces. This means that the contribution of the SM impedance to the EM impedance is negligibly small as compared to the two peak resonant-frequency responses. Note that the impedance signatures in those frequency ranges are associated with the SM impedance responses of the PZT interfaces and the tendon-anchorage system (see Eq. (2.1)). Therefore, it is needed to prove that the two peak frequencies are related to the PZT interfaces' structural properties (e.g., material, geometrical and boundary conditions). It is also needed to prove that the two peak frequencies are changed due to the change of the tendon forces.

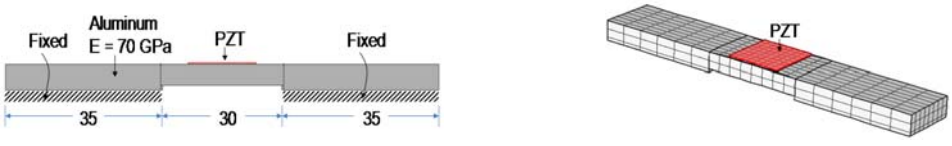

(a) Boundary condition (b) Meshing solid elements
Figure 4.1 FE Model of mountable PZT interface

A finite element (FE) model of the PZT interface is established by the commercial package, COMSOL Multiphysics. Figure 4.1(a) shows the geometry and the fixed-fixed boundary condition of the PZT interface. The selection of the fixed boundary condition was based on the fact that the flexural stiffness of the PZT interface is much smaller than that of the bearing plate, as stated previously. In FE modeling, the interface was

discretized by 3D elastic solid elements, as shown in Figure 4.2(b). The meshing includes 608 solid elements: 64 elements for the PZT patch and 544 elements for the interface body. The properties of the aluminum interface are specified for the FE model (Huynh et al. 2014). Also, the PZT patch is added by the piezoelectric material, PZT-5A (eFunda, 2010). To acquire the EM impedance responses, a harmonic excitation voltage with an amplitude of 1 V was simulated to the top surface of the PZT patch element, and the bottom one was set as the ground electrode.

4.2. Local Dynamic Responses of Two Interfaces

Impedance responses of the two PZT interfaces were numerically analyzed, as shown in Figure 4.2. The numerical impedance responses of the two interfaces were consistent as compared to the experimental impedance responses, as shown in Figure 3.1. Interface 1 shows the first and second peak frequencies at 20.44 kHz and 82.27 kHz, respectively. Interface 2 shows the first and second peaks of impedance responses at 19.18 kHz and 38.44 kHz, respectively. The first peaks of the two interfaces are very close in their frequencies; meanwhile, the second peaks of them are quite different from each other. It is noted that the second peak is reduced from 82.27 kHz to 38.44 kHz as the width of the interface is increased from 18 mm to 33 mm (see Fig. 2.2(a)).

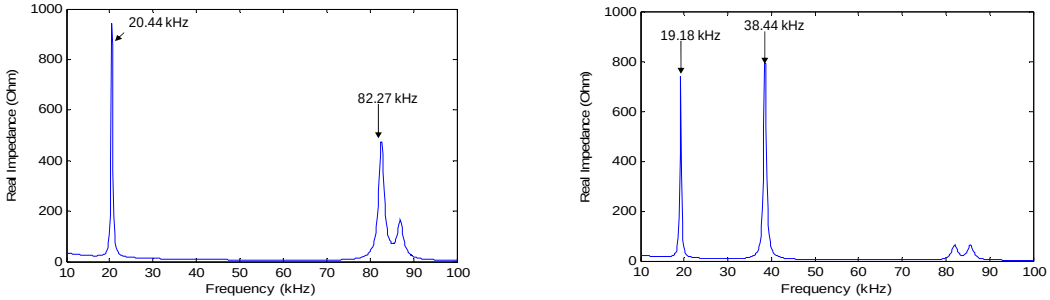

(a) Interface 1 (b) Interface 2

Figure 4.2 Numerical impedance responses of two PZT interfaces

4.2.1. Modal analysis of Interface 1

Numerical modal analyses were performed for Interface 1. The first eight mode shapes representing the local vibration responses of Interface 1 were obtained as shown in Figure 4.3. Among them, modes 1, 4 and 5 are out-of-plane longitudinal flexural motions. Modes 2, 6, and 7 are out-of-plane longitudinal twist motions. Mode 3 is an in-plane lateral bending motion. Mode 8 is an out-of-plane lateral flexural motion. Matching to the piezoelectric deformations of the PZT patch on the interface (as illustrated in Fig. 2.4), the first longitudinal flexural motion (mode 1) is identical to the first impedance peak that represents the first resonant frequency. Also, the first lateral flexural motion (mode 8) is identical to the second impedance peak that represents the second resonant frequency. From the comparison between Fig. 4.2 and Fig. 4.3, two modal shapes of Interface 1 corresponding to the two resonant impedance peaks were numerically analyzed as 20.366 kHz (mode 1) and 81.527 kHz (mode 8), respectively. It is observed that the first and second peaks of the impedance responses are identical to the modes (i.e., modes 1 and 8) that represent the local vibration responses of the Interface 1.

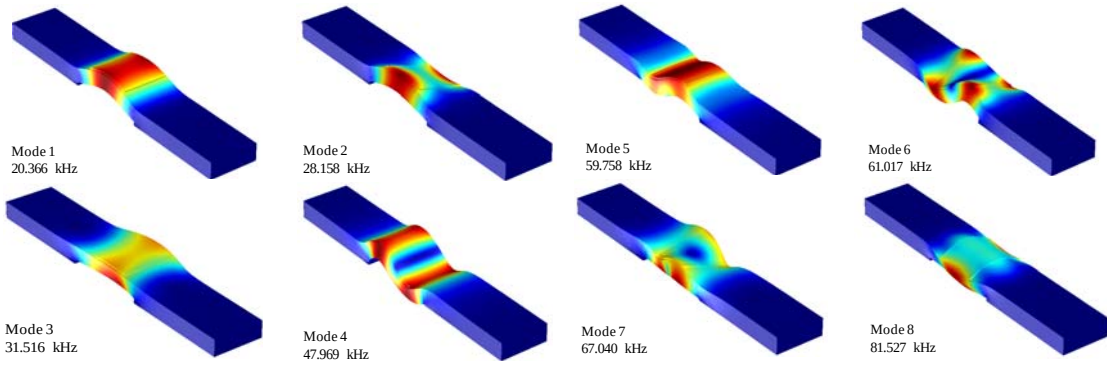

Figure 4.3 Interface 1's eight modal shapes corresponding to resonant impedance frequencies

4.2.2. Modal analysis of Interface 2

Next, numerical modal analyses were also performed for Interface 2. The first four mode shapes representing the local vibration responses of Interface 2 were obtained as shown in Fig. 4.4. Among them, mode 1 is an out-of-plane longitudinal flexural motion. Mode 2 is an out-of-plane longitudinal twist motion. Mode 3 is an in-plane lateral bending motion. Mode 4 is out-of-plane lateral flexural motion. Matching to the piezoelectric deformations of the PZT patch on the interface (as illustrated in Fig. 2.4), the first longitudinal flexural motion (mode 1) is identical to the first impedance peak that represents the first resonant frequency. Also, the first lateral flexural motion (mode 4) is identical to the second impedance peak that represents the second resonant frequency. From the comparison, two modal shapes of Interface 2 corresponding to the two resonant impedance peaks were numerically analyzed as 19.016 kHz (mode 1) and 37.923 kHz (mode 4), respectively. It is observed that the first and second peaks of the impedance responses are identical to the modes (i.e., modes 1 and 4) that represent the local vibration responses of Interface 2. It is also observed from the two interfaces that the second modal frequencies matching to the second impedance peaks are reduced from 81.527 kHz to 37.923 kHz as the interface's widths are increased from 18 mm (Interface 1) to 33 mm (Interface 2) as shown in Fig. 2.2(a).

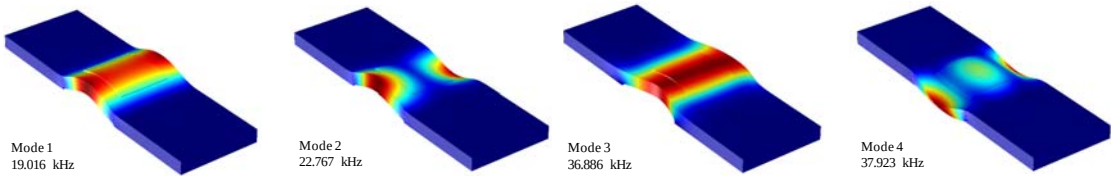

Figure 4.4 Interface 1's eight modal shapes corresponding to resonant impedance frequencies

4.3. Modal Sensitivity Analyses of Two Interfaces

Modal sensitivities of the two PZT interfaces are estimated by using an eigenvalue sensitivity concept proposed by Kim and Stubbs (1995). Suppose p^*_j is an unknown parameter of the j^{th} member of a structure for which M eigenvalues ($\omega^2_{i,m}$, i = 1,...,M) are known. Also, suppose p_j is a known parameter of the j^{th} member of a FE model for which the corresponding set of M eigenvalues ($\omega^2_{i,a}$, i = 1,...,M) are known. Then the modal sensitivity, S_{ij}, of the i^{th} eigenvalue $\omega^2_{i,a}$ with respect to the j^{th} structural parameter p_j is defined as follows:

$$S_{ij} = \frac{\delta\omega^2_{i,a}}{\delta p_j}\frac{p_j}{\omega^2_{i,a}} \tag{4.1}$$

where δp_j is the first order perturbation of p_j which produces the variation in eigenvalue $\delta\omega^2_{i,a}$. As shown in Fig. 4.1, the FE model consisted of two member types by regrouping the 544 solid elements of the interface body (as shown in Figure 4.1): member 1 (the two outside contact bodies) and member 2 (the inside flexural beam). The structural parameters of the two members are noted as p_1 and p_2, respectively. Initial values for the geometric properties of the FE model were estimated as the same values as those used for the modal analyses of the PZT interfaces.

4.3.1. Modal sensitivity of Interface 1

A FE model was designed for the geometry and boundary conditions of Interface 1. The modal sensitivity matrix was estimated as follows: firstly, two damage scenarios were introduced into the FE model; secondly, two eigenvalues of mode 1 and mode 8 (shown in Fig. 4.4) were calculated; thirdly, the fractional changes of the two eigenvalues were computed and modal sensitivity matrix was computed as listed in Table 4.1. In Member 1 (i.e., the two outside contact bodies), the first mode's sensitivity was much higher than the eighth mode's sensitivity on the structural change (e.g., change in contact boundary condition). In Member 2 (i.e., the inside flexural beam), the sensitivity of the eighth mode was relatively higher than that of the first mode. Overall, modal sensitivities of Member 2 were much higher than those of Member 1. This indicates that any changes in structural parameters of Member 2 dominate the variation of dynamic characteristics of Interface 1.

4.3.2. Modal sensitivity of Interface 2

Another FE model was established for the geometry and boundary conditions of Interface 2. The modal sensitivity matrix was estimated by the same process used for Interface 1, as shown in Table 4.1. Similarly, in Member 1 (i.e., the two outside contact bodies), the sensitivity of the first mode was much higher than that of the fourth mode on the structural change (e.g., change in contact boundary condition). In Member 2 (i.e., the

inside flexural beam), the fourth mode's sensitivity was relatively higher to the first mode's one. Generally, modal sensitivities of Member 2 were much higher than those of Member 1. It is noted that the change in structural parameters of Member 2 dominates the variation of dynamic characteristics of Interface 2. It is also noted that the modal sensitivities of Interface 2 are relatively stable than those of Interface 1.

Table 4.1 Modal Sensitivity of Interfaces 1 and 2

Peak	Interface 1		Interface 2	
	Member 1	Member 2	Member 1	Member 2
1	0.2819	0.7181	0.2401	0.7599
2	0.0478	0.9522	0.0952	0.9048

4. CONCLUDING REMARKS

From the experimental tests on the two interfaces, at least three major results were observed as follows: firstly, the impedance responses measured via the two interfaces had two dominant peaks which were sensitive to the change of prestress forces; secondly, the sensitive frequency ranges were shifted as the geometry and boundary condition of the interface were changed; and finally, the PZT interface with the larger bonding area revealed much higher sensitivity for the indication of the prestress-loss. From the analyses of dynamic characteristics of the mountable interfaces, at least four main results were observed as follows: firstly, there existed vibration modal shapes (longitudinal flexural and lateral flexural motions) which were matching to piezoelectric responses (longitudinal and lateral deformations) of the PZT patch on the interface; secondly, the second modal frequencies of the two interfaces matching to the second impedance peaks of them were reduced as the interface's widths were increased; thirdly, the change in structural parameters of the inner flexural section of the interface dominated the variation of dynamic characteristics which were corresponding to the change in impedance responses of the interface; and finally, the modal sensitivities of the PZT interface with the larger bonding area were relatively stable.

AKCNOWLEDGEMENT

This work was supported by Basic Science Research Program through the National Research Foundation of Korea (NRF) funded by the Ministry of Education, Science and Technology (NFR-2013R1A1A2A10012040). Graduate students involved in this research were also supported by the Brain Korea 21 Plus program of Korean Government.

REFERENCES

1. Bhalla, S. and Soh, C.K. (2003), "Structural Impedance Based Damage Diagnosis by Piezo-Transducers", *Earthquake Engineering and Structural Dynamics*, **32:12**, 1897-1916.
2. Huynh, T.C. and Kim, J.T. (2014), "Impedance-Based Cable Force Monitoring in Tendon-Anchorage using Portable PZT-Interface Technique", *Mathematical Problems in Engineering*, **2014**, 11 pages.
3. Huynh, T.C., Park, Y.H., Park, J.H., and Kim, J.T. (2014), "Feasibility Verification of Mountable PZT-Interface for Impedance Monitoring In Tendon-Anchorage", *Shock and Vibration*, **2014**, Article ID 262975, 11 pages.
4. Kim, J.T., Park, J.H., Hong, D.S. and Park, W.S. (2010), "Hybrid Health Monitoring of Prestressed Concrete Girder Bridges by Sequential Vibration-Impedance Approaches", *Engineering Structures*, **32**, 115-128.
5. Kim, J.T. and Stubbs, N. (1995). "Model-Uncertainty Impact and Damage-Detection Accuracy in Plate Girder", *Journal of Structural Engineering*, **121:10**, 1409–1417.
6. Liang, C., Sun, F.P., and Rogers, C.A. (1996), "Electro-Mechanical Impedance Modeling Of Active Material Systems", *Smart Materials and Structures*, **5:2**, 171-186.
7. Mascarenas, D.L., Todd, M.D., Park, G. and Farrar, C.R. (2007), "Development of an Impedance-Based Wireless Sensor Node for Structural Health Monitoring", *Smart Materials and Structures*, **16:6**, 2137-2145.
8. Nguyen, K. D., and Kim, J.T. (2012), "Smart PZT-Interface For Wireless Impedance-Based Prestress-Loss Monitoring In Tendon-Anchorage Connection", *Smart Structures and Systems*, **9:6**, 489-504.
9. Zagrai, A. N.and Giurgiutiu, V. (2001), "Electro-Mechanical Impedance Method for Crack Detection in Thin Plates", *Journal of Intelligent Material Systems and Structures*, **12**, 709-718.
10. Efunda, Inc. (2010), http://www.efunda.com